Engineered biosynthesis of β-alkyl tryptophan analogs

Christina E. Boville[+], Remkes A. Scheele[+], Philipp Koch, Sabine Brinkmann-Chen, and Andrew R. Buller*, Frances H. Arnold*

Abstract: Non-canonical amino acids (ncAAs) with dual stereocenters at the α and β positions are valuable precursors to natural products and therapeutics. Despite the potential applications of such bioactive β-branched ncAAs, their availability is limited due to the inefficiency of the multi-step methods used to prepare them. Here we report a stereoselective biocatalytic synthesis of β-branched tryptophan analogs using an engineered variant of *Pyrococcus furiosus* tryptophan synthase (*Pf*TrpB), *Pf*TrpB^{7E6}. *Pf*TrpB^{7E6} is the first biocatalyst to synthesize bulky β-branched tryptophan analogs in a single step, with demonstrated access to 27 ncAAs. The molecular basis for the efficient catalysis and broad substrate tolerance of *Pf*TrpB^{7E6} was explored through X-ray crystallography and UV-visible light spectroscopy, which revealed that a combination of active-site and remote mutations increase the abundance and persistence of a key reactive intermediate. *Pf*TrpB^{7E6} provides an operationally simple and environmentally benign platform for preparation of β-branched tryptophan building blocks.

Amino acids are nature's premier synthetic building blocks for bioactive molecules. Alongside the standard proteinogenic amino acids are diverse non-canonical amino acids (ncAAs) that are structurally similar but are not ribosomally incorporated into proteins. Due to the presence of functional groups that confer novel chemical and biological properties,[1] ncAAs can be found in natural products and 12% of the 200 top-grossing pharmaceuticals.[2,3] Of interest are β-branched ncAAs, which possess a chiral center at the β-position in addition to the standard chirality at the α-position of an amino acid **(Figure 1a)**. The two adjacent stereocenters impose conformational constraints that affect the biochemical properties of both the amino acids themselves and the molecules they compose.[4–7] These properties make β-branched ncAAs frequent components of useful natural products, biochemical probes, and therapeutics **(Figure 1b)**.[8–13] Despite their broad utility, most β-branched ncAAs are not readily available due to the challenge of forming two adjacent stereocenters while tolerating the reactive functional groups present in amino acids.[14–18] For example, traditional organic synthesis of (2*S*, 3*S*)-β-methyltryptophan (β-MeTrp) requires multiple steps that incorporate protecting groups, hazardous reagents, and expensive metal catalysts.[19,20] To take full advantage of these bioactive molecules, an improved methodology is needed to synthesize β-branched ncAAs.

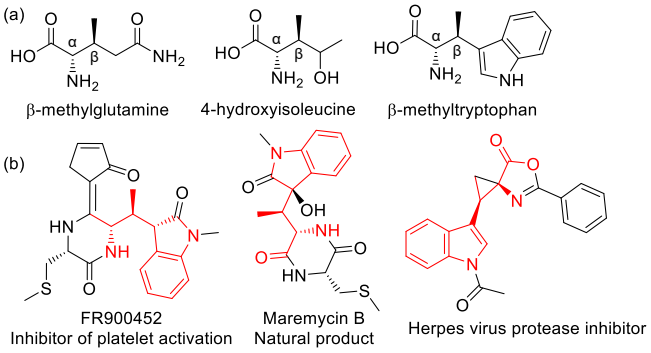

Figure 1. Representative β-branched amino acids. (a) Examples of β-branched ncAAs. (b) Examples of products derived from β-branched tryptophan analogs (red).

Enzymes offer an efficient and sustainable alternative to chemical synthesis and are routinely used to generate enantiopure amino acids from simple materials without the need for protecting groups.[21] Although several classes of enzymes have been employed in this pursuit, those using the pyridoxal phosphate cofactor (PLP, vitamin B6) are among the most prominent.[22] The most common biocatalytic route to an amino acid requires a fully assembled carbon skeleton and a PLP-dependent transaminase which is used to set the stereochemistry. However, as with traditional organic methodologies, the enzymatic synthesis of β-branched ncAAs is often confounded by the presence of a second stereocenter. The capacity to incorporate biocatalytic C–C bond-forming steps *en route* to diverse β-branched ncAAs would therefore be a powerful synthetic tool.

Few β-branched ncAA synthases have been reported, and even more rare are enzymes that produce branches larger than a methyl group. We previously engineered the β-subunit of the PLP-dependent enzyme tryptophan synthase from the thermophilic archaeon *Pyrococcus furiosus* (*Pf*TrpB) as a stand-alone ncAA synthase able to generate tryptophan (Trp) analogs from serine (Ser) and the corresponding substituted indole **(Figure 2a)**.[23–25] Further engineering of *Pf*TrpB for improved C–C bond formation with indole analogs and threonine (Thr) led to *Pf*TrpB^{2B9} (eight mutations from wild-type *Pf*TrpB), which exhibited a >1,000-fold improvement in (2*S*, 3*S*)-β-methyltryptophan (β-MeTrp) production relative to wild type **(Figure 2b)**.[26,27] While the reactive amino-acrylate intermediate (E(A-A)) **(Figure 3a)** readily forms with Thr, mechanistic analysis showed that competing hydrolysis of (E(A-A)) resulted in abortive deamination that consumed the amino acid substrate **(Figure 3b),**[28,29] limiting the enzyme's yield (typically < 50%) with a single equivalent of Thr. Further, *Pf*TrpB^{2B9} accepted only Ser and Thr as substrates since larger β-alkyl substrates were unable to efficiently form E(A-A).

[a] Dr. C. E. Boville, R. A. Scheele, P. Koch, Dr. S. Brinkmann-Chen, Prof. F. H. Arnold
Division of Chemistry and Chemical Engineering 210-41, California Institute of Technology, 1200 East California Boulevard, Pasadena, California 91125, United States
Email: frances@cheme.caltech.edu
[b] Prof. A. R. Buller
Department of Chemistry, University of Wisconsin, 1101 University Avenue, Madison, WI 53706, United States
Email: arbuller@wisc.edu
[+] These authors contributed equally to this work.

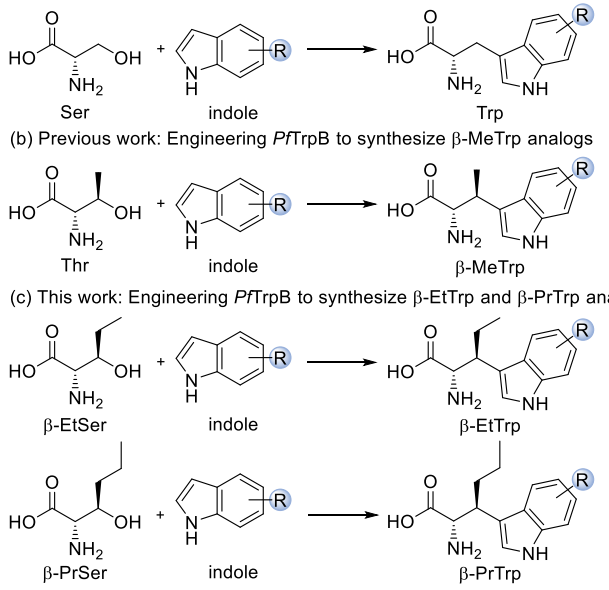

Figure 2. Synthesis of Trp and Trp analogs by *Pf*TrpB.

To surmount these challenges, we sought to identify mutations that would facilitate formation of E(A-A) with the more challenging (2*S*, 3*R*)-β-ethylserine (β-EtSer) and (2*S,* 3*R*)-β-propylserine (β-PrSer) substrates while simultaneously decreasing E(A-A) hydrolysis **(Figure 2c)**. The latter is essential, as increasingly bulky alkyl chains are thought to hinder nucleophilic attack. Increased E(A-A) persistence will allow more time for the intrinsically slower addition reaction to occur while reducing the amount of starting material lost to competing hydrolysis **(Figure 3b)**.

We chose *Pf*TrpB^{2B9} as our engineering starting point to increase production of β-EtTrp. While an active catalyst with Thr, *Pf*TrpB^{2B9} was sluggish with β-EtSer (80 total turnovers, TTN) and gave too little signal for high-throughput screening.[23] We speculated that active-site mutations would promote the formation of E(A-A) with larger, sterically demanding β-substituents and used a structure-guided approach to improve activity with β-EtSer. Modeling β-EtSer into the *Pf*TrpB^{2B9} active site as E(A-A) (PDB: 5VM5)[30] suggested a steric clash with L161 **(Figure 4a)**. Hypothesizing that this constraint could be reduced by mutating L161 to a residue with a smaller side chain **(Figure 4b)**, we expressed and assayed variants *Pf*TrpB^{2B9} L161V, L161A, and L161G. We found that L161V and L161A increased the TTN 14-fold and 10-fold, respectively, whereas L161G decreased activity by a factor of 2.6 **(Figure 4c)**. As our long-term interest is to produce a catalyst that accommodates a wider range of β-alkyl chains, we selected *Pf*TrpB^{2B9} L161A as the parent enzyme for directed evolution, with the rationale that the smaller sidechain of alanine would minimize steric clashes with bulkier substrates.

We then introduced random mutations into the *Pf*TrpB^{2B9} L161A gene and screened for enhanced β-EtTrp synthesis **(Table 1)** at 290 nm under saturating substrate conditions.[23] Screening made use of starting materials containing a mixture of diastereomers, however only the (2*S*,3*R*) diastereomer underwent a productive reaction. High-throughput screening of 352 variants yielded *Pf*TrpB^{0E3} (L91P), which displayed a 43-fold increase in TTN for β-EtTrp **(Figure 4d)**. *Pf*TrpB^{0E3} was then used as the parent for a second round of random mutagenesis, yielding variant *Pf*TrpB^{8C8} (V173E), which improved β-EtTrp yields by 54-fold relative to *Pf*TrpB^{2B9}. At this juncture, a third round of random mutagenesis failed to yield further improvements after screening 880 variants. Although the accumulated mutations increased activity, we speculated that further improvements were hindered by deleterious mutations that reduced enzyme stability.[31] We therefore recombined mutations in TrpB^{8C8}, allowing a 50% chance for each residue to retain the mutation or revert to wild type. Recombination included all residues except those which were crucial for starting activity with Ser (T292S), Thr (F95L), and β-EtSer (L161A and L91P) **(Table S1)**. Recombination also included F274L, which was previously identified as an activating mutation.[23] Recombined variants were assayed for β-EtTrp production at 290 nm, which revealed that I68V and T321A were non-essential, but that F274L was beneficial, yielding variant *Pf*TrpB^{7E6}. Though *Pf*TrpB^{7E6} did not show improved stability **(Table S2)**, recombination did enhance activity, with a 58-fold

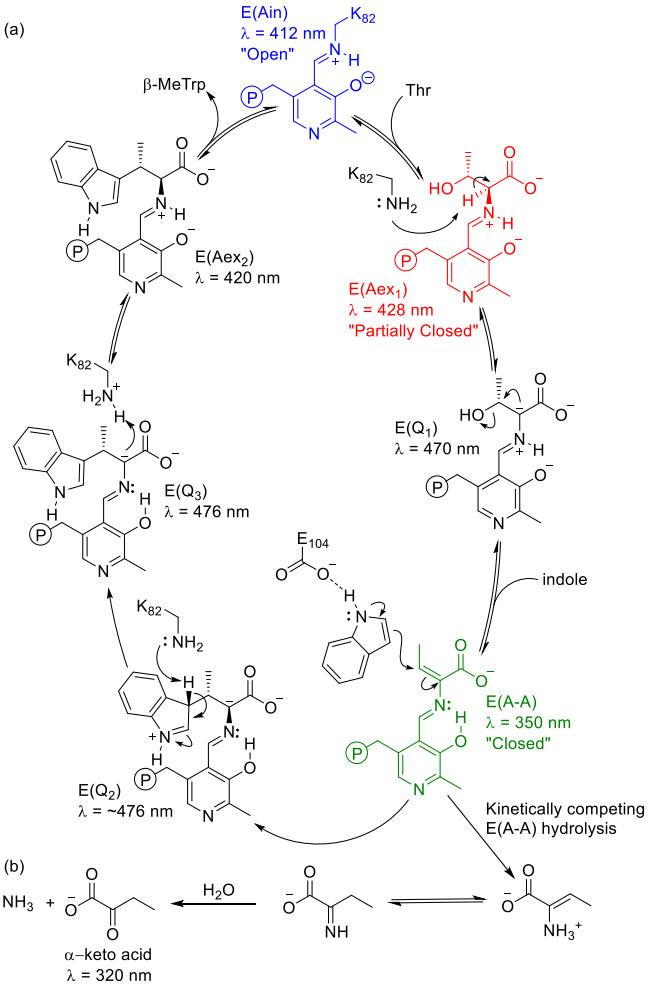

Figure 3. The putative catalytic cycle for *Pf*TrpB synthesizing β-MeTrp. (a) Catalysis initiates as E(Ain) with the mobile COMM domain predominantly in the open conformation (blue). With the addition of Thr, the COMM domain undergoes rigid body motion, transitioning to a partially closed position through E(Aex$_1$) (red) followed by full closure with formation of the reactive E(A-A) intermediate (green). E(A-A) is then attacked by indole and undergoes an addition reaction to form β-MeTrp. (b) E(A-A) may also undergo a kinetically competing hydrolysis reaction to generate α-keto acids, observable at 320 nm. This deamination reaction consumes an equivalent of the amino acid substrate.

improvement relative to *Pf*TrpB^{2B9} **(Figure 4d)**. An additional round of recombination sampled other previously identified activating mutations (Q38R, M139L, N166D, S335N) and allowed for reversion of L91P. This process produced a variant (*Pf*TrpB^{2G8}, see **Table 1**) that lacked the L91P mutation and had only slightly lower activity than *Pf*TrpB^{7E6}. Although subsequent work showed that *Pf*TrpB^{2G8} is also a proficient enzyme (vide infra), the parent *Pf*TrpB^{7E6} was selected for mechanistic characterization as it is a comparatively simple catalyst with excellent activity and more amenable to crystallization.

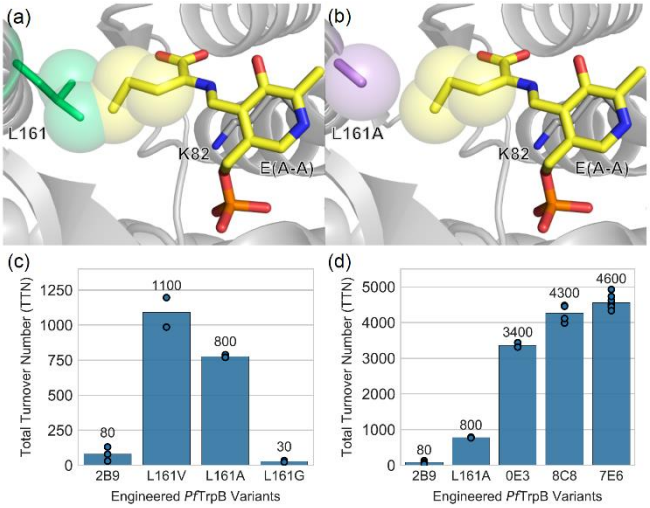

Figure 4. Engineering *Pf*TrpB for β-EtTrp synthesis. (a) β-EtSer as E(A-A) (yellow) modeled in the *Pf*TrpB^{2B9} (PDB: 5VM5, gray) active site. Spheres represent the Van der Waals radii and highlight a clash with L161 (green). (b) As in (a), but with the mutation L161A shown (purple). (c) β-EtTrp production by *Pf*TrpB^{2B9} with L161V, L161A, or L161G mutations. (d) β-EtTrp production by engineered *Pf*TrpB variants. Bars represent the average of all data points, with individual reactions shown as circles. At minimum, reactions were performed in duplicate.

We sought to identify which newly evolved properties of *Pf*TrpB enabled increased TTNs with challenging β-branched substrates. As described above, the activity and substrate scope of the parent enzyme, *Pf*TrpB^{2B9}, were limited by low steady-state population (abundance) and subsequent breakdown (persistence) of the reactive E(A-A) intermediate.[27] To assess the abundance of E(A-A), we capitalized on the intrinsic spectroscopic properties of the PLP cofactor to visualize the steady-state distribution of intermediates throughout the catalytic cycle **(Figure 3a)**.[32] With the addition of β-EtSer to *Pf*TrpB^{7E6}, the internal aldimine peak (E(Ain), 412 nm) decreased and E(A-A) (350 nm) became the major species **(Figure 5a)**. This is a notable change, as when β-EtSer was added to *Pf*TrpB^{2B9}, E(Aex$_1$) accumulated and no E(A-A) was observed **(Fig 5a)**. To assess the persistence of E(A-A), we assayed the deamination rate and coupling efficiency of *Pf*TrpB^{7E6}. In the presence of both Thr and β-EtSer, *Pf*TrpB^{7E6} displayed up to a 4-fold decrease in the deamination reaction relative to *Pf*TrpB^{2B9} **(Table S3)**. We then probed the enzyme's coupling efficiency under reaction conditions with high catalyst loading and equimolar substrate equivalents, where product formation is limited only by the consumption of starting material through the competing deamination reaction. We observed an increase in product formation from 5% with *Pf*TrpB^{2B9} to 96% with *Pf*TrpB^{7E6} when β-EtSer was the substrate **(Figure 5b)**. Collectively, these data

Table 1. Engineering *Pf*TrpB through directed evolution for improved β-EtTrp production. Engineering began with *Pf*TrpB^{2B9} (*Pf*TrpB I16V, E17G, I68V, F95L, F274S, T292S, T321A, and V384A) with 80 TTN. All reactions were performed in at least duplicate with 0.1% catalyst loading for 24 hours at 75 °C.

Variant	Mutations Added	Mutations Removed	Average TTN
[a]*Pf*TrpB^{2B9} L161A	L161A	N/A	800
[b]*Pf*TrpB^{0E3}	L91P	N/A	3400
[b]*Pf*TrpB^{8C8}	V173E	N/A	4300
[c]*Pf*TrpB^{7E6}	F274L	I68V, T321A	4600
[c]*Pf*TrpB^{2G8}	M139L, N166D, S335N	L91P	3800

[a] Site-directed mutagenesis. [b] Random mutagenesis. [c] Recombination.

indicate that increased product formation was achieved by incorporating mutations that facilitate the formation of E(A-A) and increase its lifetime in the active site.

During directed evolution, *Pf*TrpB was altered by the introduction of nine mutations. Although *Pf*TrpB^{7E6} has only a single mutation in the active site **(Figure S1)**, mutations governing enzyme activity are scattered throughout the protein.[23,33] Remote mutations may be affecting the enzyme's conformational dynamics, which have been previously shown to be linked to the catalytic cycle of *Pf*TrpB **(Figure 3a)**.[30,33] In its resting state, *Pf*TrpB binds PLP via the catalytic lysine (K82) as E(Ain) with the mobile communication (COMM) domain in a predominantly open conformation. Addition of an amino acid substrate induces formation of the external aldimine (E(Aex$_1$)), which is accompanied by partial closure of the COMM domain. Dehydration to form the electrophilic E(A-A) species occurs when TrpB populates a fully closed conformation, where it remains until product is formed.[28,29] To examine the state of the *Pf*TrpB^{7E6} active site and its connection to the COMM domain conformational cycling, we determined the X-ray crystal structures of *Pf*TrpB^{7E6} in the E(Ain) state as well as with β-EtSer bound in the active site as E(A-A).

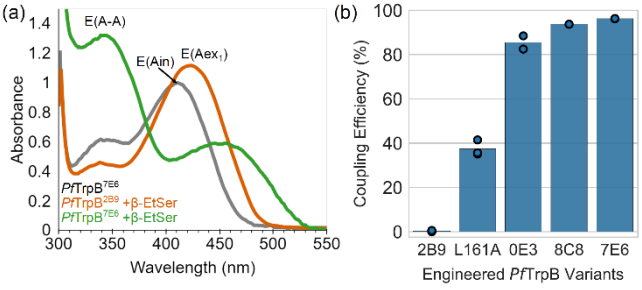

Figure 5. Directed evolution stabilizes E(A-A) and improves coupling efficiency. (a) The steady-state population of *Pf*TrpB as determined by UV-visible light spectroscopy. In the absence of substrate, the predominant population of *Pf*TrpB^{7E6} (black) is E(Ain). β-EtSer-bound *Pf*TrpB^{2B9} (orange) accumulates E(Aex$_1$) and *Pf*TrpB^{7E6} (green) forms E(A-A). All spectra are normalized to the absorbance value of E(Ain) at 412 nm. (b) Variant coupling efficiency with β-EtSer. Bars represent the average of all data points, with individual reactions shown as circles. At minimum, reactions were performed in duplicate.

Earlier *Pf*TrpB variants, including *Pf*TrpB^{2B9}, were nearly identical to wild-type *Pf*TrpB (PDB: 5DVZ) in the open state. Here, the 2.26-Å structure of *Pf*TrpB^{7E6} (PDB: 6CUV) shows distinct preorganization toward a more closed conformation. Specifically,

in half of the protomers, the COMM domain has shifted into a distinct partially-closed conformation that was previously associated with substrate binding **(Figure 6a)**. While many residues may contribute to the stabilization of this state, we hypothesize that the mutation L91P destabilizes open states; this residue lies on an α-helix immediately prior to the COMM domain in the sequence and causes a kink in the helix that shifts the structure toward more closed states **(Figure 6b)**.

We next soaked *Pf*TrpB^{7E6} with β-EtSer and obtained a 1.75-Å structure with β-EtSer bound as E(A-A) in two protomers (PDB: 6CUZ). As expected, the COMM domain underwent rigid-body motion to the closed conformation **(Figure 6a)** where the steric complementarity between the longer β-alkyl chain and L161A becomes apparent. Notably, the L161A mutation does not appear to induce significant alterations elsewhere in the active site **(Figure 6c).** When indole is modeled into the active site, there is space to accommodate even longer β-branched substituents as well as a range of indole nucleophiles **(Figure 6d)**.

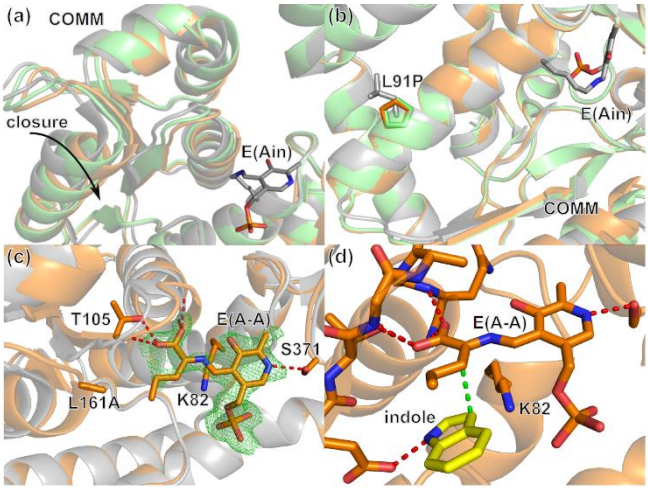

Figure 6. Substrate binding and conformational changes in *Pf*TrpB. (a) The COMM domain of *Pf*TrpB undergoes rigid body motion that is linked to the catalytic cycle. In the absence of substrate, wild-type *Pf*TrpB (PDB: 5DVZ, gray) is in the open conformation, while *Pf*TrpB^{7E6} (PDB: 6CUV, green) assumes a partially closed conformation. When β-EtSer is bound to *Pf*TrpB^{7E6} as E(A-A) (PDB: 6CUV, orange), the COMM domain undergoes a rigid body shift to a closed conformation. (b) The mutation L91P introduces a kink in the α-helix adjacent to the COMM domain. (c) β-EtSer bound to *Pf*TrpB^{7E6} as E(A-A) is shown with F_o-F_c map contoured at 2.0σ (green). The gamma carbon of the amino-acrylate is not well resolved. Hydrogen bonds are shown as red dashes. (d) Indole (yellow) modeled in the active site of *Pf*TrpB^{7E6} with β-EtSer as E(A-A). The green dash represents the bond-forming atoms in indole and β-EtSer.

As our goal was to evolve a versatile β-branched ncAA synthase, we next explored the substrate scope of *Pf*TrpB^{7E6}. We hypothesized that, if improvements in activity came through increased stability of E(A-A), the same mutations should increase activity with multiple amino acid substrates. Indeed, we found that although we screened for β-EtTrp synthesis, the TTN for β-MeTrp and (2*S,* 3*S*)-β-propyltryptophan (β-PrTrp) synthesis were simultaneously improved 3.6-fold and 36-fold, respectively **(Figure 7a)**. Consistent with our previous observations, directed evolution improved the enzyme's coupling efficiency **(Figure 7b)** and amino-acrylate persistence **(Figure 7c-d)** with all three acid substrates. Next, we revisited our earlier hypothesis that the L161A mutation would be more beneficial than L161V by reducing steric clashes with larger substrates. We observed that although *Pf*TrpB^{7E6} L161V is viable for synthesis of β-MeTrp and β-EtTrp, the TTN for β-PrTrp formation was reduced 5-fold **(Figure S2a)**. In addition, *Pf*TrpB^{7E6} retained the robust Trp activity that is the hallmark of the wild-type enzyme **(Figure S2b)**, demonstrating that the L161A mutation was successful in accommodating bulkier substrates, allowing catalysis with four different amino acid substrates.

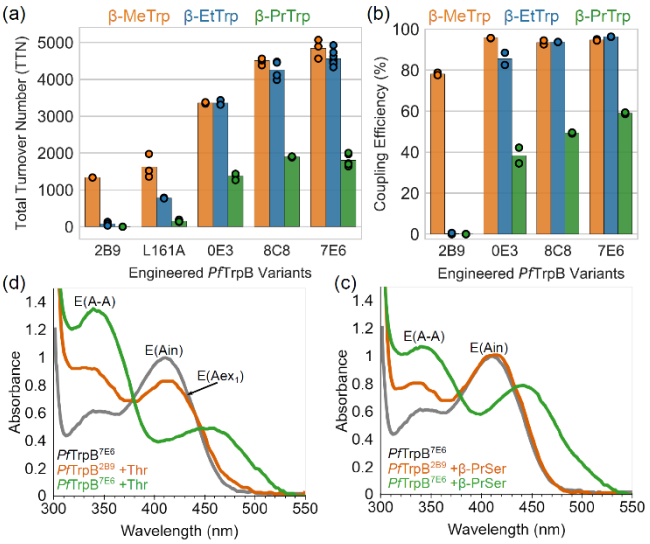

Figure 7. *Pf*TrpB engineering grants access to a range of β-branched tryptophan analogs. (a) TTN of *Pf*TrpB for β-MeTrp (orange), β-EtTrp (blue), and β-PrTrp (green). (b) Variant coupling efficiency with Thr (orange), β-EtSer (blue), and β-PrSer (green). Bars represent the average of all data points, with individual reactions shown as circles. At minimum, reactions were performed in duplicate. (c) The steady-state population of *Pf*TrpB with Thr as determined by UV-visible light spectroscopy. In the absence of substrate, the predominant population of *Pf*TrpB^{7E6} (black) is E(Ain). With the addition of Thr to *Pf*TrpB^{2B9} (orange) has a mixed population of E(Aex$_1$) and E(A-A), while *Pf*TrpB^{7E6} (green) is predominantly E(A-A). (d) β-PrSer-bound *Pf*TrpB^{2B9} (orange) remains as E(Ain) while *Pf*TrpB^{7E6} (green) predominantly forms E(A-A).

However, activity was not observed with all β-alkyl substrates and reactions with (2*S*)-β-isopropylserine (β-iPrSer) showed only trace activity. To understand why catalysis did not proceed with this bulkier sidechain, we soaked β-iPrSer into *Pf*TrpB^{7E6} crystals and obtained a 1.77-Å structure (PDB: 6CUT), which shows the catalytically unreactive (2*S*, 3*S*) diastereomer of β-iPrSer bound as E(Aex$_1$) **(Figure S3)**. Though (2*S*, 3*S*)-β-iPrSer can form E(Aex$_1$), dehydration across the C_α–C_β bond requires a rotameric shift of the side chain that we hypothesize is hindered by steric interactions with an adjacent loop.[34] Further work is needed to understand whether the poor activity of *Pf*TrpB^{7E6} with (2*S,* 3*R*)-β-iPrSer reflects inhibition by an isomeric analog, increased allylic strain of the amino-acrylate, or a combination of effects.

In addition to acting on multiple amino acid substrates, we hypothesized that *Pf*TrpB^{7E6} would retain the wild-type enzyme's breadth of reactivity with indole analogs.[23–25] We performed analytical biotransformations with 11 representative nucleophiles with three β-branched amino acid substrates, yielding 27 tryptophan analogs, 20 of which are previously unreported **(Table 2)**. Each reaction was analyzed by liquid-chromatography/mass spectrometry (LCMS) and TTN were calculated by comparing product and substrate absorption at the isosbestic wavelength **(Table S4)**. Happily, we found that substituted indole analogs

Table 2. β-Branched tryptophan analogs synthesized by *Pf*TrpB^{7E6}. Average TTN (10,000 max TTN) are indicated for each combination of amino acid and nucleophile substrate. At minimum, reactions were performed in duplicate. See Supplemental Information for experimental details.

Electrophilic Substrate	Nucleophilic Substrate: Indole	2-methylindole	4-methylindole	4-fluoroindole	5-methylindole	5-fluoroindole	5-chloroindole	6-methylindole	7-methylindole	7-azaindole	Indazole
Thr	4800	4500	1000	4500	800	5800	<100	1400	3000	4800	200
β-EtSer	4600	3000	700	1600	100	3700	N.D.	700	2800	N.D.	N.D.
β-PrSer	1800	200	100	200	<100	400	N.D.	100	1100	N.D.	N.D.

remained well-tolerated by *Pf*TrpB^{7E6}. Methyl substituents were accepted around the indole ring, though the enzyme demonstrated higher activity with fluoroindoles. We also observed activity with 5-chloroindole and Thr, a reaction that was undetectable for the parent enzyme, *Pf*TrpB^{2B9}. In addition, we have abolished the undesirable *N*-alkylation reaction that occurred with *Pf*TrpB^{2B9} in the presence of 7-azaindole and 4-fluorindole.[27] However, yields with *N*-nucleophilic substrates such as indazole remained low with β-branched substrates relative to their Ser counterparts. Importantly, *Pf*TrpB^{7E6} can synthesize these ncAAs using only a single equivalent of the amino acid substrate, whereas *Pf*TrpB^{2B9} had required 10 equivalents. This is a testament to the value of improving the stability of the reactive E(A-A) intermediate in the reaction.

All product identities were confirmed by ^{1}H- and ^{13}C-NMR as well as high-resolution mass spectrometry from 100-µmol preparative reactions using two equivalents of electrophilic substrate. Reactions were conducted at 0.01 to 0.4 mol% catalyst loading, and we found that, under these conditions, *Pf*TrpB^{7E6} maintained robust activity: β-MeTrp with 6,600 TTN (88% yield), β-EtTrp with 6,200 TTN (82% yield), and β-PrTrp with 2,100 TTN (84% yield). We also used the recombination variant *Pf*TrpB^{2G8} **(Table 1)** to synthesize and characterize 27 tryptophan analogs on a preparative scale **(Table S5)**. For future applications, reactions may be further optimized by tuning catalyst loading and increasing substrate equivalents **(Table S6)**. In conjunction with the high expression levels of *Pf*TrpB^{7E6} (~300 mg enzyme per L culture), a range of β-branched ncAAs are now accessible on a preparative scale. We have developed a new biocatalytic route to (2*S*, 3*S*)-tryptophan analogs using the engineered thermostable catalyst, *Pf*TrpB^{7E6}. Through directed evolution, we increased the abundance and persistence of the key E(A-A) intermediate by the introduction of active-site and remote mutations. In turn, *Pf*TrpB^{7E6} displays improved coupling efficiency with multiple β-branched amino acid substrates.

This work significantly extends previous efforts to engineer *Pf*TrpB enzymes, which have proven to be versatile and efficient catalysts for production of tryptophan analogs.

Acknowledgements

The authors thank Dr. David Romney, Patrick Almhjell, Dr. Christopher Prier, Nathaniel Goldberg, and Ella Watkins for their helpful discussions and comments on the manuscript. We thank Dr. Jens Kaiser of the Caltech Molecular Observatory, Dr. Scott Virgil and the Center for Catalysis and Chemical Synthesis, and Dr. Mona Shahgholi and Naseem Torian from the Caltech Mass Spectrometry Laboratory. This work was funded by the Jacobs Institute for Molecular Medicine (Caltech) and the Rothenberg Innovation Initiative. C.E.B. was supported by a postdoctoral fellowship from the Resnick Sustainability Institute. R.A.S. was supported by funding from the University of Groningen.

Keywords: biocatalysis • tryptophan synthase • non-canonical amino acid • β-branched amino acid • directed evolution

[1] F. Agostini, J.-S. Völler, B. Koksch, C. G. Acevedo-Rocha, V. Kubyshkin, N. Budisa, *Angew. Chem. Int. Ed.* **2017**, *56*, 9680–9703.
[2] N. A. McGrath, M. Brichacek, J. T. Njardarson, *J. Chem. Educ.* **2010**, *87*, 1348–1349.
[3] M. A. T. Blaskovich, *Journal of Medicinal Chemistry* **2016**, *59*, 10807–10836.
[4] S. E. Gibson (née Thomas), N. Guillo, M. J. Tozer, *Tetrahedron* **1999**, *55*, 585–615.
[5] V. J. Hruby, *J. Med. Chem.* **2003**, *46*, 4215–4231.
[6] V. W. Cornish, M. I. Kaplan, D. L. Veenstra, P. A. Kollman, P. G. Schultz, *Biochemistry* **1994**, *33*, 12022–12031.
[7] C. Haskell-Luevano, L. W. Boteju, H. Miwa, C. Dickinson, I. Gantz, T. Yamada, M. E. Hadley, V. J. Hruby, *J. Med. Chem.* **1995**, *38*, 4720–4729.
[8] C. Milne, A. Powell, J. Jim, M. Al Nakeeb, C. P. Smith, J. Micklefield, *J. Am. Chem. Soc.* **2006**, *128*, 11250–11259.
[9] J. C. Sheehan, D. Mania, S. Nakamura, J. A. Stock, K. Maeda, *J. Am. Chem. Soc.* **1968**, *90*, 462–470.
[10] Y. Zou, Q. Fang, H. Yin, Z. Liang, D. Kong, L. Bai, Z. Deng, S. Lin, *Angew. Chem. Int. Ed.* **2013**, *52*, 12951–12955.
[11] J. Michaux, G. Niel, J.-M. Campagne, *Chem. Soc. Rev.* **2009**, *38*, 2093.
[12] S. Takase, N. Shigematsu, I. Shima, I. Uchida, M. Hashimoto, T. Tada, S. Koda, Y. Morimoto, *J. Org. Chem.* **1987**, *52*, 3485–3487.
[13] I. L. Pinto, A. West, C. M. Debouck, A. G. DiLella, J. G. Gorniak, K. C. O'Donnell, D. J. O'Shannessy, A. Patel, R. L. Jarvest, *Bioorganic Med. Chem. Lett.* **1996**, *6*, 2467–2472.
[14] S. G. Davies, A. M. Fletcher, A. B. Frost, J. A. Lee, P. M. Roberts, J. E. Thomson, *Tetrahedron* **2013**, *69*, 8885–8898.
[15] S.-Y. Zhang, Q. Li, G. He, W. A. Nack, G. Chen, *J. Am. Chem. Soc.* **2013**, *135*, 12135–12141.
[16] M. J. O'Donnell, J. T. Cooper, M. M. Mader, *J. Am. Chem. Soc.* **2003**, *125*, 2370–2371.
[17] C. Xiong, W. Wang, C. Cai, V. J. Hruby, *J. Org. Chem.* **2002**, *67*, 1399–1402.
[18] S. Lou, G. M. McKenna, S. A. Tymonko, A. Ramirez, T. Benkovics, D. A. Conlon, F. González-Bobes, *Org. Lett.* **2015**, *17*, 5000–5003.
[19] Y. Sawai, M. Mizuno, T. Ito, J. Kawakami, M. Yamano, *Tetrahedron* **2009**, *65*, 7122–7128.

[20] L. Jeannin, M. Boisbrun, C. Nemes, F. Cochard, M. Laronze, E. Dardennes, Á. Kovács-Kulyassa, J. Sapi, J.-Y. Laronze, *Comptes Rendus Chim.* **2003**, *6*, 517–528.
[21] Y.-P. Xue, C.-H. Cao, Y.-G. Zheng, *Chem. Soc. Rev.* **2018**, *47*, 1516–1561.
[22] M. L. Di Salvo, N. Budisa, R. Contestabile, *Beilstein Bozen Symp. Mol. Eng. Control* **2012**, 27–66.
[23] A. R. Buller, S. Brinkmann-Chen, D. K. Romney, M. Herger, J. Murciano-Calles, F. H. Arnold, *Proc. Natl. Acad. Sci. U.S.A.* **2015**, *112*, 14599–14604.
[24] D. K. Romney, J. Murciano-Calles, J. E. Wehrmüller, F. H. Arnold, *J. Am. Chem. Soc.* **2017**, *139*, 10769–10776.
[25] J. Murciano-Calles, D. K. Romney, S. Brinkmann-Chen, A. R. Buller, F. H. Arnold, *Angew. Chem. Int. Ed.* **2016**, *55*, 11577–11581.
[26] A. R. Buller, P. van Roye, J. Murciano-Calles, F. H. Arnold, *Biochemistry* **2016**, *55*, 7043–7046.
[27] M. Herger, P. van Roye, D. K. Romney, S. Brinkmann-Chen, A. R. Buller, F. H. Arnold, *J. Am. Chem. Soc.* **2016**, *138*, 8388–8391.
[28] B. G. Caulkins, B. Bastin, C. Yang, T. J. Neubauer, R. P. Young, E. Hilario, Y. M. Huang, C. A. Chang, L. Fan, M. F. Dunn, et al., *J. Am. Chem. Soc.* **2014**, *136*, 12824–12827.
[29] B. G. Caulkins, R. P. Young, R. A. Kudla, C. Yang, T. J. Bittbauer, B. Bastin, E. Hilario, L. Fan, M. J. Marsella, M. F. Dunn, et al., *J. Am. Chem. Soc.* **2016**, *138*, 15214–15226.
[30] A. R. Buller, P. van Roye, J. K. B. Cahn, R. A. Scheele, M. Herger, F. H. Arnold, *J. Am. Chem. Soc.* **2018**, *140*, 7256–7266.
[31] J. D. Bloom, S. T. Labthavikul, C. R. Otey, F. H. Arnold, *Proc. Natl. Acad. Sci. U.S.A.* **2006**, *103*, 5869–5874.
[32] W. F. Drewe, M. F. Dunn, *Biochemistry* **1986**, *25*, 2494–2501.
[33] M. F. Dunn, *Arch. Biochem. Biophys.* **2012**, *519*, 154–166.
[34] E. W. Miles, D. R. Houck, H. G. Floss, *J. Biol. Chem.* **1982**, *257*, 14203–14210.